

# Frequency evaluation of UTC(NPL) by NPL-Sr1 for the period MJD 60129 to 60154

National Physical Laboratory

August 3, 2023

The secondary frequency standard NPL-Sr1 and an optical frequency comb were used to evaluate the frequency of UTC(NPL) over a period of 25 days from MJD 60129 to MJD 60154 (4<sup>th</sup> July 2023 – 29<sup>th</sup> July 2023). The Sr optical lattice clock operation covers 46.9% of the total measurement period. The result of the evaluation is reported in table 1 and is made using the CCTF 2021 recommended frequency value for the  $5s^2\ ^1S_0 - 5s5p\ ^3P_0$  unperturbed optical transition in  $^{87}\text{Sr}$ : 429 228 004 229 872.99 Hz with a relative standard uncertainty of  $u_{\text{Srep}} = 1.9 \times 10^{-16}$  [1].

Period of estimation	$y(\text{UTC(NPL)} - \text{NPL-Sr1}) / 10^{-16}$	$u_A / 10^{-16}$	$u_B / 10^{-16}$	$u_{A/\text{Lab}} / 10^{-16}$	$u_{B/\text{Lab}} / 10^{-16}$	$u_{\text{Srep}} / 10^{-16}$	Uptime
MJD 60129–60154	-1.91	0.004	0.120	3.33	1.97	1.9	46.9%

Table 1: Results of the evaluation of UTC(NPL) by NPL-Sr1.

## 1 Measurement configuration

NPL-Sr1 was operated as described in reference [2], with the exception of some changes described in section 2 below. The 698 nm clock laser was pre-stabilized to a local reference cavity and then phase-locked via a fibre-based optical frequency comb to another more stable laser at 1064 nm. A feedback loop acting on an acousto-optic modulator (AOM) kept the clock laser frequency in resonance with the  $^{87}\text{Sr}$  clock transition.

Following a change in the reference maser for UTC(NPL) in January 2021, and a subsequent redistribution of reference frequency signals within NPL in February 2021, the optical frequency comb was no longer referenced to UTC(NPL), but instead to a separate maser reference HM6.

The frequency ratio between the  $^{87}\text{Sr}$  clock transition and HM6 was calculated from the comb measurements of the 698 nm ultrastable laser and the AOM frequency corrections. The frequency ratio was determined as the midpoint of a weighted linear fit to the NPL-Sr1/HM6 ratio data. The time offset between HM6 and UTC(NPL) was continually measured by an SR620 time interval logger. By taking the derivative of this time offset we determined the mean frequency difference between the two signals over the evaluation period. This was then combined with the frequency comb measurements to obtain the frequency ratio between the  $^{87}\text{Sr}$  clock transition and UTC(NPL). HM6 was not steered during this evaluation period.

Systematic effect	Correction / $10^{-18}$	Uncertainty / $10^{-18}$
BBR chamber	4952.0	11.4
BBR oven	0.5	0.5
Quadratic Zeeman	221.6	0.3
Lattice	-5.0	2.2
Collisions	0.0	0.8
Background gas	6.4	1.0
DC Stark	0.016	0.016
Probe Stark	0.0	1.0
Servo Error	0.0	0.0
<b>Total Correction</b>	5175.5	11.7
Gravitational redshift	-1215.0	2.7
<b>Total including gravitational redshift</b>	3960.5	12.0

Table 2: Uncertainty budget for the NPL-Sr1 lattice clock for this evaluation period. Reported uncertainties correspond to 68% confidence intervals. This table applies to the period MJD 60129–60154.

## 2 NPL-Sr1 evaluation

### Type A uncertainty

The type A uncertainty  $u_A$  is the statistical contribution from the frequency instability of NPL-Sr1. This was estimated based on a white frequency noise component of  $4.5 \times 10^{-16}/\sqrt{\tau}$ , extrapolated to the duration of the evaluation period.

This is an improvement compared to the earlier reports covering the periods MJD 58659–58679 ( $5 \times 10^{-16}/\sqrt{\tau}$ ), MJD 58454–58459 ( $8 \times 10^{-16}/\sqrt{\tau}$ ) and MJD 57904–57919 and MJD 57929–57934 ( $2 \times 10^{-15}/\sqrt{\tau}$ ). The improvement is a direct result of improvements made to the 1064 nm laser to which the 698 nm clock laser is stabilised. The stability was evaluated by interleaved measurements.

### Type B uncertainty

The type B uncertainty  $u_B$  is the sum in quadrature of the systematic uncertainty of NPL-Sr1 and the uncertainty of the gravitational redshift relative to the conventionally adopted reference potential  $W_0 = 62\,636\,856.0 \text{ m}^2\text{s}^{-2}$ .

The systematic frequency corrections and uncertainty budget for NPL-Sr1 for the period of this report are given in table 2. The geopotential value for NPL-Sr1 is taken from [3].

The uncertainty in table 2 is lower than that of the uncertainty evaluation published in reference [2]. For this reason, the value of  $u_B$  in table 1 is increased to the published value that has undergone peer review.

Changes to the uncertainty evaluation presented in reference [2] are described below.

### *Blackbody radiation*

In this report we continue to use the updated dynamic correction coefficient for blackbody radiation, reported in reference [4]. The methodology to evaluate our blackbody radiation correction remains as in [2].

### *Quadratic Zeeman*

For this evaluation, we continued using a nominal stretched state splitting of 640 Hz (similar to that used in reference [2] and in the prior reported periods MJD 60034–60064 and 60064–60079). We continue to use the updated value for the quadratic Zeeman shift coefficient of  $-2.456(3) \times 10^{-7} \text{ Hz}^{-1}$  [5].

### *Background Gas*

As for the previous evaluations, we use an updated coefficient for the background gas collisional shift of  $(-3.0 \pm 0.3) \times 10^{-17}/\tau$ , where  $\tau$  is the  $1/e$  vacuum-limited trap lifetime [6]. Assuming hydrogen is the dominant gas in our system we arrive at a shift of  $(-6.4 \pm 1.0) \times 10^{-18}$  based on a lattice trapped lifetime measurement of 4.7 s (re-evaluated after breaking vacuum for replacement of the Zeeman slowing beam viewport). Unlike previous reports where the gas composition was unknown, an evaluation of the residual gas content of the vacuum shows hydrogen as dominant and so we assign a total uncertainty for the shift of  $1.0 \times 10^{-18}$  which is a combination of the coefficient and vacuum lifetime measurement uncertainties.

### *Collisions*

We use the cold collisional shift re-evaluation from the previous reporting period MJD 60064 - 60094.

### *Lattice*

The same lattice conditions as in the prior reported period MJD 60034–60064 were operated throughout this evaluation period.

## 3 Frequency comparison

### Type A uncertainty

The uncertainty  $u_{\text{A/Lab}}$  arises mainly from the dead time in the comparison between HM6 and NPL-Sr1, and includes both a deterministic correction due to maser drift and a stochastic contribution (table 3).

The stochastic contribution was estimated by a method described in [7]. This involves a Monte-Carlo approach where the frequency noise of HM6 is simulated and a value calculated for the offset between the mean frequency during the uptime periods and the mean frequency during the whole evaluation period. The simulation was repeated 1000 times, with the standard deviation of the offsets providing an estimate for the frequency uncertainty arising from the dead times in the operation of NPL-Sr1.

Contribution	Uncertainty / $10^{-18}$
$u_{\text{A/Lab}}$ [Deterministic]	5
$u_{\text{A/Lab}}$ [Stochastic]	332
$u_{\text{A/Lab}}$ [HM6-UTC(NPL)]	13
$u_{\text{A/Lab}}$ [Total]	333

Table 3: A breakdown of the uncertainties included in  $u_{\text{A/Lab}}$ .

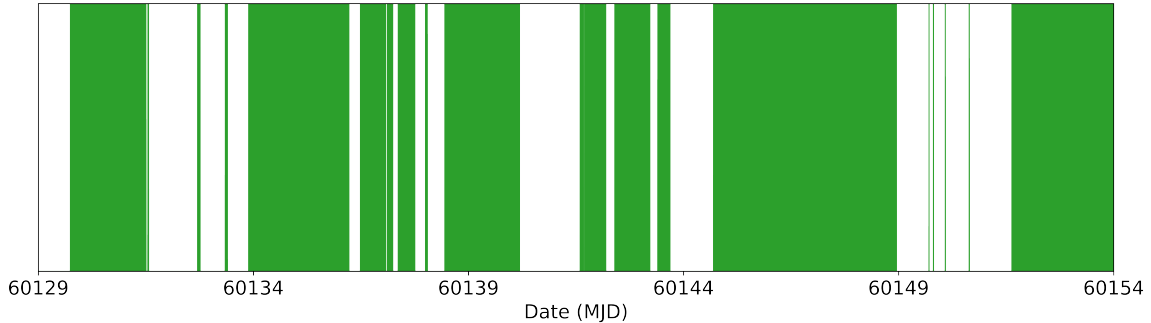


Figure 1: Uptime of NPL-Sr1 over the evaluation period (green regions).

The maser noise model used comprised white phase noise of  $1.00 \times 10^{-13}/\tau$ , white frequency noise of  $5.40 \times 10^{-14}/\sqrt{\tau}$ , a flicker frequency floor of  $1.25 \times 10^{-15}$  and a random-walk frequency component of  $2.55 \times 10^{-19}\sqrt{\tau}$ . In addition, maser HM6 exhibits periodic frequency fluctuations that were estimated as an additional noise process proportional to the sum of three sinusoids in the simulated noise, with amplitudes  $4.0 \times 10^{-15}$ ,  $3.0 \times 10^{-15}$  and  $3.5 \times 10^{-15}$  and periods  $3 \times 10^4$  s,  $8.64 \times 10^4$  s and  $1.728 \times 10^5$  s respectively. These values were derived from measurements of HM6 by NPL-Sr1 during the evaluation period.

For this evaluation period, NPL-Sr1 had an uptime of 46.9%, distributed as shown in figure 1.

The SR620 time interval logger that links HM6 to UTC(NPL) introduces an additional contribution to  $u_{A/Lab}$ , which is computed from the statistical spread of the time interval measurements.

### Type B uncertainty

The most significant contribution to the uncertainty  $u_{B/Lab}$  is the distribution of the 10 MHz signal from HM6 to the frequency comb laboratory, and the subsequent synthesis in that laboratory of an 8 GHz signal against which the repetition rate of the frequency comb was measured. Potential phase fluctuations were monitored using a loop-back comparison as described in reference [2], and their contribution to the uncertainty estimated from the instability of these fluctuations over the evaluation period.

The SR620 time interval logger that links HM6 to UTC(NPL) also contributes to  $u_{B/Lab}$ . This contribution is estimated based on the specification of the instrument.

Contribution	Uncertainty / $10^{-18}$
$u_{B/Lab}$ [Distribution]	194
$u_{B/Lab}$ [HM6-UTC(NPL)]	33
<b><math>u_{B/Lab}</math>[Total]</b>	197

Table 4: A breakdown of the uncertainties included in  $u_{B/Lab}$ .

## References

- [1] Consultative Committee for Time and Frequency (CCTF), “[Recommendation PSFS-2 from the 22nd meeting \(session II – online\)](#),” (2022).
- [2] R. Hobson, W. Bowden, A. Vianello, A. Silva, C. F. A. Baynham, H. S. Margolis, P. E. G. Baird, P. Gill, and I. R. Hill, “A strontium optical lattice clock with  $1 \times 10^{-17}$  uncertainty and measurement of its absolute frequency,” *Metrologia* **57**, 065026 (2020).
- [3] F. Riedel, A. Al-Masoudi, E. Benkler, S. Dörscher, V. Gerginov, C. Grebing, S. Häfner, N. Hunte-mann, B. Lipphardt, C. Lisdat, E. Peik, D. Piester, C. Sanner, C. Tamm, S. Weyers, H. Denker, L. Timmen, C. Voigt, D. Calonico, G. Cerretto, G. A. Costanzo, F. Levi, I. Sesia, J. Achkar, J. Guéna, M. Abgrall, D. Rovera, B. Chupin, C. Shi, S. Bilicki, E. Bookjans, J. Lodewyck, R. L. Targat, P. Delva, S. Bize, F. N. Baynes, C. F. A. Baynham, W. Bowden, P. Gill, R. M. Godun, I. R. Hill, R. Hobson, J. M. Jones, S. A. King, P. B. R. Nisbet-Jones, A. Rolland, S. L. Shemar, P. B. Whibberley, and H. S. Margolis, “Direct comparisons of European primary and secondary frequency standards via satellite techniques,” *Metrologia* **57**, 045005 (2020).
- [4] C. Lisdat, S. Dörscher, I. Nosske, and U. Sterr, “Blackbody radiation shift in strontium lattice clocks revisited,” *Phys. Rev. Research* **3**, L042036 (2021).
- [5] T. Bothwell, D. Kedar, E. Oelker, J. M. Robinson, S. L. Bromley, W. L. Tew, J. Ye, and C. J. Kennedy, “JILA SrI optical lattice clock with uncertainty of  $2.0 \times 10^{-18}$ ,” *Metrologia* **56**, 065004 (2019).
- [6] B. X. R. Alves, Y. Foucault, G. Vallet, and J. Lodewyck, “Background Gas Collision Frequency Shift on Lattice-Trapped Strontium Atoms,” in *2019 Joint Conference of the IEEE International Frequency Control Symposium and European Frequency and Time Forum (EFTF/IFC)* (IEEE, Orlando, FL, USA, 2019) pp. 1–2.
- [7] D.-H. Yu, M. Weiss, and T. E. Parker, “Uncertainty of a frequency comparison with distributed dead time and measurement interval offset,” *Metrologia* **44**, 91 (2007).